Available online at www.sciencedirect.com

SciVerse ScienceDirect

Ceramics International 39 (2013) 5453–5458

CERAMICS INTERNATIONAL

www.elsevier.com/locate/ceramint

Hydrothermal synthesis of zeolite Rho using methylcellulose as the space-confinement additive

Xu Liu[a], Xianghong Zhang[a], Zongpeng Chen[b], Xiaoyao Tan[a,*]

[a]*The State Key Laboratory of Hollow Fabre Membrane Materials and Processes, Department of Chemical Engineering, Tianjin Polytechnic University, Tianjin 300387, China*

[b]*Shanghai Stuff Science & Technology Co. Ltd., Shanghai 201506, China*

Received 18 November 2012; received in revised form 17 December 2012; accepted 17 December 2012
Available online 26 December 2012

Abstract

Pure zeolite Rho has been synthesized by the hydrothermal method using CsOH and 18-crown-6 ether as the template agent and methylcellulose (MC) as the space-confinement additive. XRD, SEM, FT-IR and TGA-DTA techniques were applied to characterize the obtained zeolite Rho powders. The results indicate that the addition of MC is able to promote the overall crystallization rate of zeolite Rho and simultaneously to control the particles to a size smaller than 1 μm and a uniform size distribution. However, a higher calcination temperature, i.e. around 600 °C is also required to remove the water and organic species occluded in the zeolite precursor.

Keywords: Zeolite Rho; Hydrothermal synthesis; Space-confinement; Crystallization

1. Introduction

Zeolite Rho is a small pore size (3.6 × 3.6 Å) aluminosilicate zeolite with a low Si/Al ratio (2.5–3). It has a structure consisting of a body-centered cubic arrangement of α-cages linked via double 8-rings (D8R) [1]. This framework displays a considerable flexibility during the sorption–desorption process and thus is able to adapt to different cation sizes and variously shaped adsorbent molecules [2,3]. For example, the framework cation (sodium and cesium) sites can be substituted by NH_4^+, Ba^{2+}, Sr^{2+} and Cd^{2+} etc. [4]. Zeolite Rho has been applied as a highly selective catalyst in the production of dimethylamine from ammonia and methanol [5–10]. In addition, it can also serve as a hydrogen storage material after specific alternations of the size and charge of the exchangeable cations [11–13] or as a CO_2 selective adsorbent [14].

Properties of a zeolite are mainly determined by its structure and composition, but also can be influenced greatly by the synthesis process. In the earlier work, zeolite Rho is usually synthesized through the hydrothermal technique in the presence of cesium cations without using any template agents [15]. But it is difficult to obtain the pure single phase unless under the conditions of free of impurities. When the cesium cation is deficient during the synthesis or the cesium is not uniformly distributed in the gel, zeolite X (FAU) will be formed as one of the product series [16]. With the use of 18-crown-6 ether (1,4,7,10,13,16-hexaoxacyclooctadecane) as template agent, the crystallization of zeolite Rho can be promoted to form pure phase under relatively wide conditions [17,18]. Furthermore, the Si/A1 molar ratio in the zeolite framework even can be increased up to 4.5 by optimization of the synthesis parameters. Recently, pure zeolite Rho has been synthesized successfully in the absence of cesium cations using polydiallyldimethylammonium chloride (PDADMAC) as the template agent. However, it has to take 8–60 days to complete the crystallization [19]. In all these cases, the particle size of the zeolite Rho powders ranged between 3 and 10 μm depending on the aging temperature and the crystallization duration. By the use of space-confinement additives to confine zeolite crystallization in the synthesis process, the zeolite particle size can be reduced significantly, leading to the improvement of zeolite properties [20]. This confined-space synthesis method has been applied to prepare various types of nanosized zeolites such as ZSM-5, A-, X- and Y-type ones [21–23]. The space-confinement additives mainly include

*Corresponding author. Tel.: +86 22 83955663; fax: +86 22 83955663.
E-mail address: cestanxy@yahoo.com.cn (X. Tan).

0272-8842/$ - see front matter © 2012 Elsevier Ltd and Techna Group S.r.l. All rights reserved.
http://dx.doi.org/10.1016/j.ceramint.2012.12.054

Table 1
Zeolite Rho samples synthesized under different conditions.

Sample	Duration (days)	MC addition (g)	Particle size[a] (μm)	BET area ($m^2\ g^{-1}$)	Cell size (nm)	Relative crystallization[b], (%)
A-1	1	/	/		/	Amorphous
A-2	2	/	1.6	3.26	25.3	76.9
A-8	8	/	2.1	5.83	43.8	100.0
B-1	1	2	1.0	3.43	28.6	23.1
B-2	2	2	1.30	9.08	39.3	92.3
C-1	1	4	0.6	7.93	21.4	31.3
C-2	2	4	0.94	12.06	32.7	97.7

[a]Average diameter determined from SEM images.
[b]Reference to A-8, and peaks (110), (310), (411), (420), (422), (510) were taken for the calculation.

carbon black and the polymer hydrogels with three-dimensional networks created via physical or chemical cross-linking such as polyacrylamide, methylcellulose and glutaraldehyde crosslinked chitosan etc.

In this work, pure crystalline zeolite Rho with reduced particle sizes and a narrow size distribution has been synthesized by the hydrothermal method using CsOH and 18-crown-6 ether as the structure directing agent and polymer methylcellulose as the space-confinement agent. The effects of methylcellulose additive on the formation of zeolite Rho have been investigated extensively.

2. Experimental

2.1. Materials

Silica sol (SiO_2: 40 wt%, Qingdao Haiyang Chemical Co., China) and sodium aluminate ($NaAlO_2$, AR, Tianjin Gurangfu Chemical Co., China) were used as the Si and Al sources, respectively. Sodiumhydroxide (NaOH, AR) was purchased from Tianjin Fengchuan Chemical Co., China; 18-crown-6 ether (1,4,7,10,13,16-hexaoxacyclooctadecane, 18C6, AR) from Shanghai Jinchun Co., China; cesium hydroxide (CsOH, 50 wt% in water, AR) from Hubei Jieruisi New Material Co., China; and methylcellulose (MC, AR) from Tianjin Bodi Chem. Co., China.

2.2. Synthesis process

A typical synthesis procedure is described as follows. 1.35 g 18-crown-6 ether was dissolved in deionized water in a Teflon vessel followed by addition of 0.6 g NaOH and 1.8 g CsOH solution. 1.68 g sodium aluminate ($NaAlO_2$) was then added under stirring until a clear solution was formed. Thereafter, 15 g colloidal silica was added to the solution at a rate of 1.5 mL min^{-1} under stirring. Aging of the solution was carried out at room temperature for 24 h to form a white gel with a final composition of $1.8Na_2O{:}0.3Cs_2O{:}1Al_2O_3{:}l0SiO_2{:}0.5$(18-C-6):$100H_2O$ in molar ratio. A given amount of methylcellulose solution (20–40 g 10% MC in distilled water) was added with continuous stirring. Hydrothermal treatment was carried out at 110 °C for 1–8 days to complete crystallization. The crystallized solid was isolated by centrifugal separation (4000 rpm for 10 min) and washed with distilled water until pH = 10. The product was dried at 60 °C for 12 h and then calcined at 600 °C for 3 h to obtain final zeolite crystal powders. The synthesis conditions for the zeolite Rho samples are summarized in Table 1, where some calculated parameters are also listed.

2.3. Characterization

The morphology of the zeolite samples was observed using scanning electron microscopy (HITACHI S-4800). Before the measurements, the samples were coated with a layer of platinum using a platinum coater (CFC-1500, JEOL, Tokyo, Japan).

Powder diffraction data were collected at ambient temperature using a Rigaku D-max2550 X-ray diffractometer with CuKα radiation ($\lambda = 0.154056$ nm) to establish phase identity and purity. Continuous scan mode was used to collect 2θ data from 5° to 50° with a 0.01° sampling pitch and a 5 °C min^{-1} scanning rate. The X-ray tube voltage and current were set at 40 kV and 150 mA, respectively. The crystal size was calculated by the Scherrer equation:

$$d = \frac{K\lambda}{b\cos\theta}$$

where b is the full width at half maximum, $K = 0.89$, and $\lambda = 0.15406$ nm.

The framework vibration spectra of the samples were recorded by a Fourier transform infrared spectrometer (FTIR-650, Tianjin Gangdong Technological development Inc.) within the wave number range of 4000–400 cm^{-1}.

Nitrogen adsorption experiments of calcined samples were performed on a JW-BK micropore analyzer (Beijing Jingweigaobo Technological development Inc.). The BET surface areas of the samples were obtained by the multipoint Brunauer–Emmett–Teller (BET) adsorption technique.

Thermogravimetric analysis (TGA) and differential thermal analysis (DTA) were conducted using a TGA/DTA system (Diamond TG/DTA6300) with a scanning rate of 5 °C min^{-1}. 10 mg zeolite powder precursor was placed in

the sample holder and then heated from room temperature to 600 °C in air with a flow rate of 50 mL min^{-1}. The weight and the heat flux changes were recorded as a function of temperature.

3. Results and discussion

3.1. Morphology of the zeolite Rho

Fig. 1 shows the morphology of the zeolite Rho products synthesized under different conditions. For the sample obtained after 1 day's crystallization in the absence of MC additive, no distinct zeolite particles can be discriminated in the powder product (Fig. 1(A-1)). As the crystallization time was extended to 2 days, spherical zeolite particles have been formed with the average particle size of ca. 1.6 μm in diameter (Fig. 1(A-2)). This is in agreement with the observation by Araki et al. [18] who studied the crystallization process of zeolite Rho by the hydrothermal synthesis technique and found that the crystallization of zeolite Rho only started after 20 h of reaction time. However, when the MC polymer solution was added in the gel precursor, zeolite particles in cubic shape were formed within 1 day's crystallization (Fig. 1(B-1) and (C-1)), even though the relative crystallization degree is quite low, which will be discussed in more details in the below section. This indicates that the addition of MC promoted the crystallization process of zeolite Rho. Furthermore, the particle size of the formed zeolite Rho is also reduced by the use of MC additive. For example, the zeolite particles obtained after 2 days' crystallization are 1.3 μm with 2 g MC additive and 0.94 μm with 4 g MC additive in average diameter. Comparisons of B-1 with C-1 and B-2 with C-2 also suggest that although the general zeolite particle size increases with the extension of the

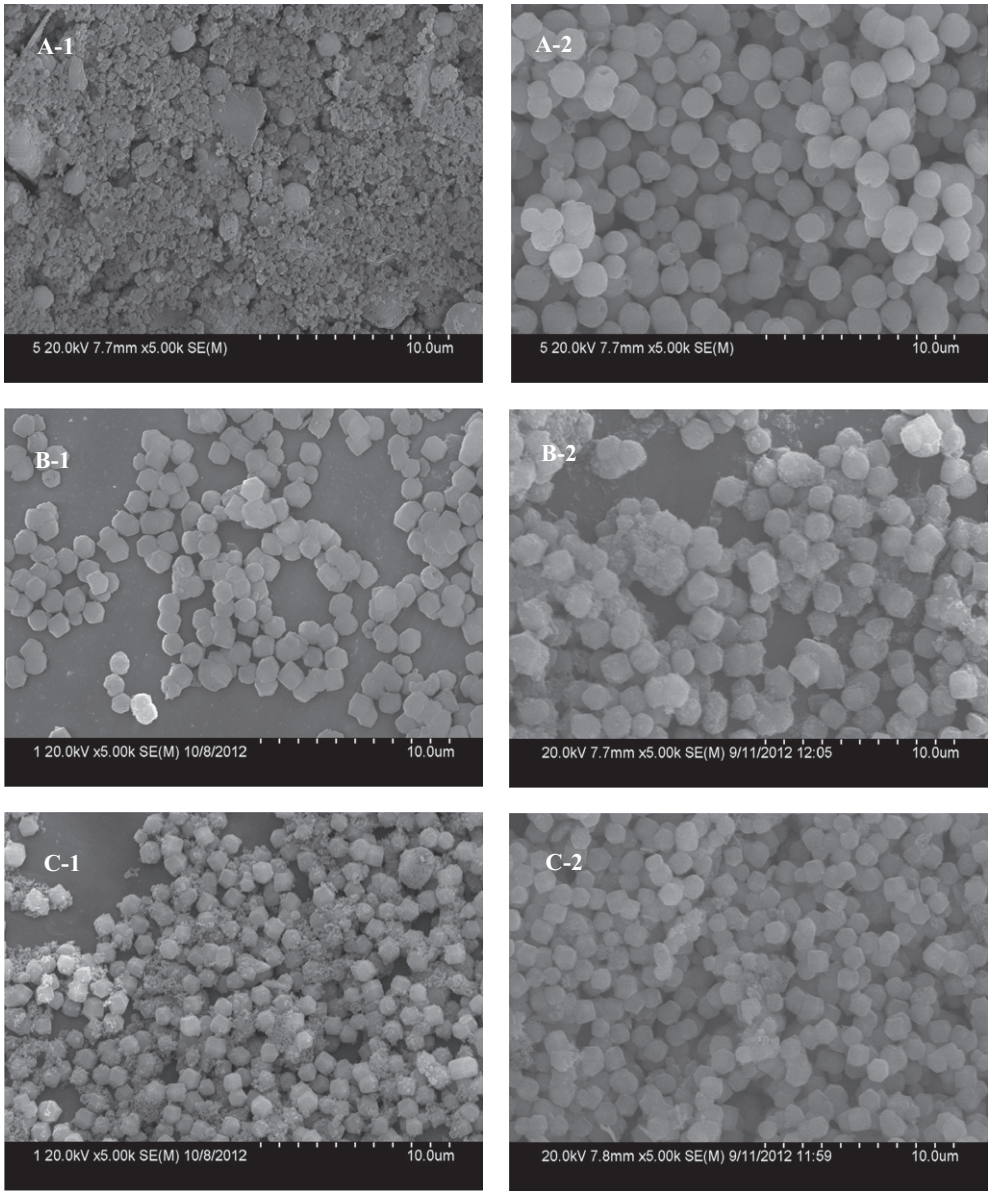

Fig. 1. SEM images of the zeolite Rho synthesized under different conditions.

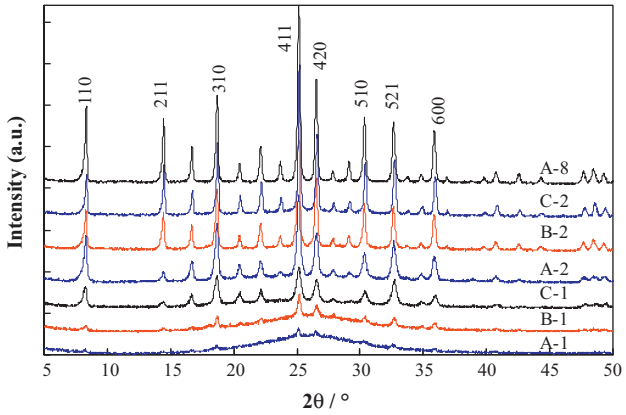

Fig. 2. XRD patterns of the zeolite Rho samples synthesized under different conditions.

crystallization time, addition of more MC can result in the formation of smaller zeolite Rho particles. These results confirm the function of MC as a space-confinement agent. As MC is dissolved in the aqueous solution, a 3D solid network will be formed. The amount of gel in each unit of the solid network is limited by its small space. Crystallization of the gel is restrained within the network unit space and the inflows of other gels around the unit can be avoided, leading to the improved overall crystallization rate. Moreover, the zeolite particle size can be smaller and more uniform as more MC additive is added in the gel solution due to the mass transfer limitation.

The BET surface areas of the sintered zeolite samples are summarized in Table 1. As can be seen, all the zeolite Rho samples possess low BET surface areas but are still larger than the literature value ($\sim 3\ m^2\ g^{-1}$). This may be attributed to the pore blocking effect of the large Cs^+ cations which are located in the double 8-ring sites [12]. Another interesting phenomenon observed is that the BET surface area is more dependent on the crystallization degree than on the particle size. For instance, the samples B-2 and C-2 have exhibited larger BET surface areas ($9.08\ m^2\ g^{-1}$ and $12.06\ m^2\ g^{-1}$, respectively) than samples B-1 ($3.43\ m^2\ g^{-1}$) and C-1 ($7.93\ m^2\ g^{-1}$) although the zeolite particle sizes are increased due to the longer crystallization duration.

3.2. Crystalline phase

Fig. 2 demonstrates the evolution of crystalline phase of zeolite Rho and the effect of MC additive on the formation of zeolite phase. As can be seen, the sample obtained after one day's crystallization in the absence of MC additive remains amorphous since no characteristic peaks of zeolite Rho have appeared on the XRD pattern. After 2 days' crystallization, all but only the characteristic diffraction peaks of zeolite Rho (PDF reference code 50–678) with the respective 2θ angles at 8.32°, 16.68°, 18.68°, 25.16°, 26.56°, 30.36°, 32.62°, and 36.86° are observed from the XRD pattern, indicating that the zeolite Rho phase has been formed without impurity. As the crystallization time was further extended to 8 days, all the characteristic diffraction peaks have become stronger, indicating that the crystallization degree has been greatly improved. As pointed out by Araki et al. [18], the formation of zeolite Rho in the hydrothermal synthesis process consists of four steps: (1) 0–3 h, dehydration and condensation reactions between silica and alumina to form amorphous aluminosilicates; (2) 3–20 h, particle growth and aggregation of amorphous aluminosilicate, which is followed by an increase in the bounding rate of the silica, alumina, and hydroxyl groups; (3) 20–48 h, crystallization and crystal growth of zeolite Rho, with a decrease in Na/Si ratio and an increase in 18-C-6 incorporation; and (4) after 48 h, gentle growth with an increase in the Na/Si ratio and a change in rate for the bounding states between the silica- and aluminum-based species. Obviously, the crystallization time cannot be less than 20 h in order to obtain complete zeolite Rho phase even though it is promoted by the use of MC polymer gel.

Although the zeolite Rho phase can be formed in the product powders after 1 day of crystallization (samples B-1 and C-1), the intensity of these characteristic diffraction peaks is lower than those obtained after longer crystallization duration. Taking the product obtained by 8 days' crystallization as the reference zeolite, the relative crystallization degree of other samples can be calculated by comparing their peak areas where the strongest peak of (110) followed by (211), (310), (411), (420) and (510) on the XRD patterns were taken into consideration. The results are summarized in Table 1. As can be seen, the crystallization degrees for samples B-1 and C-1 are only 23.1% and 31.3%, respectively. But the fact that the crystallization degree increases with increasing the amount of the MC additive in the gel solution again confirms that MC has promoted the overall crystallization rate of zeolite Rho. Furthermore, a well-expected result is that the relative crystallization degree of the zeolite Rho increases with the crystallization time. For example, samples B-2 and C-2 exhibit the relative crystallization degrees of 92.3% and 97.7%, respectively.

Applying the Scherrer equation, the crystal sizes of the zeolite Rho samples were also calculated as listed in Table 1. As can be seen, the crystal sizes of samples A-2, B-2 and C-2 are 25.3 nm, 39.3 nm and 32.7 nm, respectively. This implies that the addition of MC leads to increase of crystalline cells due to its promotion effect on the crystallization rate but decrease in particle size due to its space-confinement effect. However, the addition of MC actually favors the formation of smaller crystalline cells because the 3D network formed between the MC molecules and the hydroxide ion (–OH) limits the freely growth of the crystal surfaces [24]. As a result, the addition of more MC in the gel solution has yielded not only smaller particles but also smaller crystalline cells.

3.3. FT-IR patterns

The FT-IR peaks of zeolites can be categorized into three classes including (1) the internal vibrations of TO_4

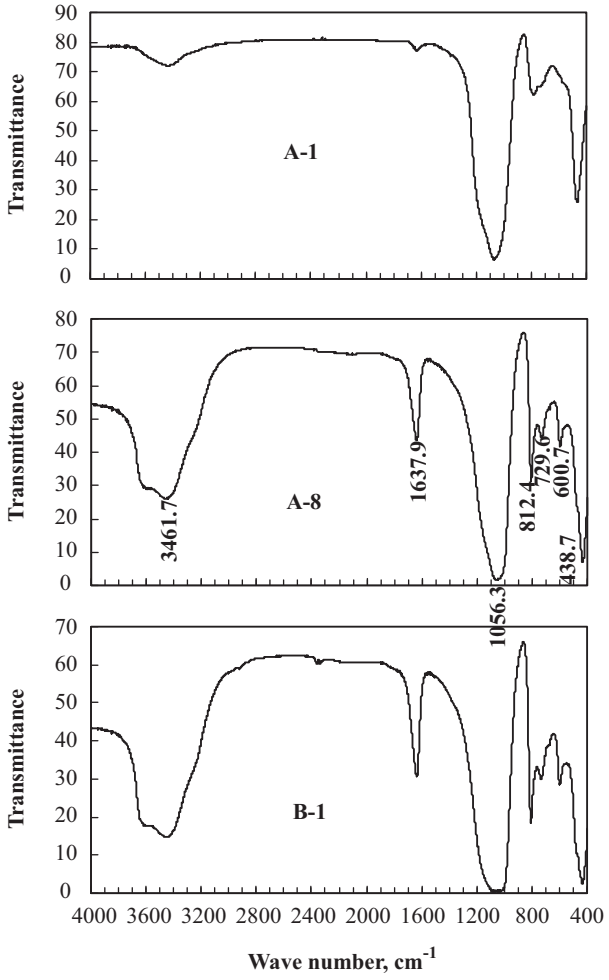

Fig. 3. FT-IR patterns of the zeolite Rho samples synthesized at different conditions.

(T=Al, Si) tetrahedron, the primary units of the zeolite Rho structure that are not sensitive to other structural vibrations; (2) the vibrations which may be related to the linkages between tetrahedral that are sensitive to the structural vibrations and (3) O–H stretching of adsorbed water and O–H bending of lattice water [25]. Fig. 3 shows the FT-IR patterns of the synthesized zeolite samples A-1, A-8 and B-1. The other samples exhibited quite similar FT-IR patterns to A-8 and would not be discussed in the following.

As can be seen from the FTIR spectra of sample A-8, the characteristic peaks appear at 438.7 cm^{-1}, 600.7 cm^{-1}, 729.6 cm^{-1}, 812.4 cm^{-1}, 1056.3 cm^{-1} 1637.9 cm^{-1} and 3461.7 cm^{-1}, which agree well with the standard IR pattern of zeolite Rho [26]. The peak at 438.7 cm^{-1} can be assigned to the internal TO_4 tetrahedral bending of the Rho zeolite structure; the peak that appeared at 600.7 cm^{-1} can be attributed to the double ring external linkage; the peaks at 729.6 cm^{-1}, 812.4 cm^{-1} and 1056.3 cm^{-1} to the symmetrical stretching of the external linkage and internal tetrahedral, while the peaks at 1637.9 cm^{-1} and 3461.7 cm^{-1} should be assigned to O–H bonding of lattice water and O–H stretching of adsorbed water, respectively. However, no peaks appear at 600.7 cm^{-1} and 729.6 cm^{-1} on the FT-IR pattern of sample A-1, indicating that the framework of zeolite Rho is not formed at this moment. In contrast, all the characteristic peaks of zeolite Rho appear on the FT-IR pattern of sample B-1. This indicates once again that the crystallization of zeolite Rho can be promoted by the addition of MC during the hydrothermal synthesis process.

3.4. TGA-DTA patterns of the zeolite precursors

In order to investigate the effect of MC additive on the synthesis of zeolite Rho, TGA-DTA curves of the zeolite precursors of samples A-2 and C-2 were measured with the results shown in Fig. 4. The TGA curves demonstrate two main stages of weight loss. For sample A-2, the first stage is from room temperature to around 125 °C with the weight loss of about 10.5%. It may be attributed to the removal of water. The second stage is from 400 °C to 480 °C accounting for the weight loss of about 5.2%, which may mainly result from the decomposition of organic species occluded in the structure. Correspondingly, on the DTA curve a small endothermic peak and an exothermic peak appear at around 89.4 °C and 465.7 °C, respectively. However, when MC additive is used, the weight loss will become slower. For example, the first main stage of weight loss for sample C-2 corresponding to the water desorption spans from room temperature to 240 °C although the weight loss is only about 8.2%. Moreover, the second main stage accounting for 9.1% weight loss spans from 280 °C to 500 °C. Therefore, the endothermic peak corresponding to the water desorption could not be distinguished on the DTA curve, but only a wide exothermic peak appears at around 420 °C reflecting the combustion of organic species. In addition, the weight of sample A-2 almost remains constant after the temperature higher than 500 °C, but for sample C-2 the weight still decreases slightly as the temperature is further increased. This implies that a higher temperature, i.e. ~600 °C is required for the calcination of zeolite precursors to remove the water and organic species when MC is used as the space-confinement additive.

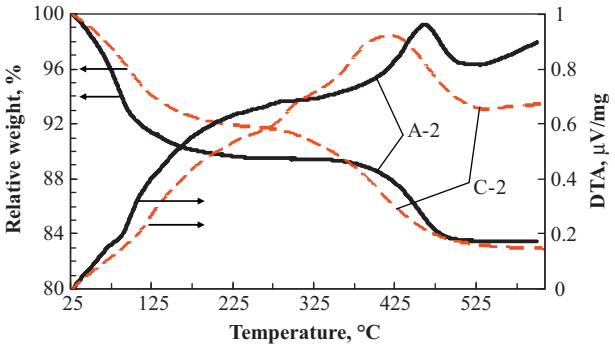

Fig. 4. TGA-DTA curves for the zeolite precursors of A-2 and C-2 samples.

4. Conclusion

Pure crystalline zeolite Rho has been successfully synthesized by the hydrothermal method using CsOH and 18-crown-6 ether as the template agent and polymer methylcellulose (MC) as the space-confinement additive. Due to the space-confinement effect of MC gel network, the particle size of zeolite Rho is controlled within 1 μm with a uniform particle size distribution. In addition, the overall crystallization rate of zeolite Rho can also be promoted leading to larger crystal size and more regulated crystal structure. However, in order to remove the water and organic species occluded in the zeolite precursors, the calcination temperature has to be increased to around 600 °C.

Acknowledgments

This work was financially supported by the Scientific and Technical Innovation Project of Tianjin Polytechnic University for graduate students.

References

[1] J.B. Parise, E. Prince, The structure of cesium-exchanged zeolite-Rho at 293 K and 493 K determined from high resolution neutron powder data, Material Research Bulletin 18 (1983) 841–852.
[2] D.R. Corbin, L. Abrams, C.A. Jones, M.M. Eddy, W.T.A. Harrison, G.D. Stucky, D.E. Cox, Flexibility of the zeolite Rho framework, in situ X-ray and neutron powder structural characterization of divalent cation-exchanged zeolite Rho, Journal of the American Chemical Society 112 (1990) 4821–4830.
[3] G.M. Johnson, B.A. Reisner, A. Tripathi, D.R. Corbin, B.H. Toby, J.B. Parise, Flexibility and cation distribution upon lithium exchange of aluminosilicate and aluminogermanate materials with the Rho topology, Chemistry of Materials 11 (1999) 2780–2787.
[4] G.M. Johnson, A. Tripathi, J.B. Parise, Synthesis and structure of a microporous aluminogermanate with the zeolite Rho topology, Microporous and Mesoporous Materials 28 (1999) 139–154.
[5] L. Abrams, D.R. Corbin, M. Keane Jr., Synthesis of dimethylamine by zeolite Rho: a rational basis for selectivity, Journal of Catalysis 126 (1990) 610–618.
[6] D.R. Corbin, S. Schwarz, G.C. Sonnichsen, Methylamines synthesis: a review, Catalysis Today 37 (1997) 71–102.
[7] L.H. Callanan, C.T. O'Connor, E. van Steen, The effect of the adsorption properties of steamed zeolite Rho on its methanol amination activity, Microporous and Mesoporous Materials 35–36 (2000) 163–172.
[8] L.H. Callanan, E. van Steen, C.T. O'Connor, Improved selectivity to lower substituted methylamines using hydrothermally treated zeolite Rho, Catalysis Today 49 (1999) 229–235.
[9] H.-Y. Jeon, C.-H. Shin, H.J. Jung, S.B. Hong, Catalytic evaluation of small-pore molecular sieves with different framework topologies for the synthesis of methylamines, Applied Catalysis A: General 305 (2006) 70–78.
[10] S. Altwasser, R. Glaser, J. Weitkamp, Ruthenium-containing small-pore zeolites for shape-selective catalysis, Microporous and Mesoporous Materials 104 (2007) 281–288.
[11] V.V. Krishnana, S.L. Suib, D.R. Corbin, S. Schwarz, G.E. Jones, Encapsulation studies of hydrogen on cadmium exchanged zeolite Rho at atmospheric pressure, Catalysis Today 31 (1996) 199–205.
[12] H.W. Langmi, A. Walton, M.M. Al-Mamouri, S.R. Johnson, D. Book, J.D. Speight, P.P. Edwards, I. Gameson, P.A. Anderson, I.R. Harris, Hydrogen adsorption in zeolites A, X, Y and Rho, Journal of Alloys and Compounds 356–357 (2003) 710–715.
[13] H.W. Langmi, D. Book, A. Walton, S.R. Johnson, M.M. Al-Mamouri, J.D. Speight, P.P. Edwards, I.R. Harris, P.A. Anderson, Hydrogen storage in ion-exchanged zeolites, Journal of Alloys and Compounds 404–406 (2005) 637–642.
[14] S. Araki, Y. Kiyohara, S. Tanaka, Y. Miyake, Adsorption of carbon dioxide and nitrogen on zeolite rho prepared by hydrothermal synthesis using 18-crown-6 ether, Journal of Colloid and Interface Science 376 (2012) 28–33.
[15] H.E. Robson, D.P. Shoemaker, R.A. Ogilvie, P.C. Manor, Molecular sieves, in: W.M. Meier, J.B. Uytterhoeven (Eds.), Advances in Chemistry Series, vol. 121, American Chemical Society, Washington, DC, 1973, pp. 106–115.
[16] L.J. Garces, V.D. Makwana, B. Hincapie, A. Sacco, S.L. Suib, Selective N,N-methylation of aniline over cocrystallized zeolites Rho and zeolite X (FAU) and over Linde type L (Sr, K-LTL), Journal of Catalysis 217 (2003) 107–116.
[17] T. Chatelain, J. Patarin, E. Fousson, M. Soulard, J.L. Guth, P. Schulz, Synthesis and characterization of high-silica zeolite RHO prepared in the presence of 18-crown-6 ether as organic template, Microporous Materials 4 (1995) 231–238.
[18] S. Araki, Y. Kiyohara, S. Tanaka, Y. Miyake, Crystallization process of zeolite rho prepared by hydrothermal synthesis using 18-crown-6 ether as organic template, Journal of Colloid and Interface Science 376 (2012) 28–33.
[19] S. Liu, P. Zhang, X. Meng, D. Liang, N. Xiao, F.-S. Xiao, Cesium-free synthesis of aluminosilicate Rho zeolite in the presence of cationic polymer, Microporous and Mesoporous Materials 132 (2010) 352–356.
[20] C. Madsen, C.J.H. Jacobsen, Nanosized zeolite crystals—convenient control of crystal size distribution by confined space synthesis, Chemical Communications 8 (1999) 673–674.
[21] S. Frisch, L.M. Röken, J. Caro, M. Wark, Ion conductivity of nano-scaled Al-rich ZSM-5 synthesized in the pores of carbon black, Microporous and Mesoporous Materials 120 (2009) 47–52.
[22] H.T. Wang, B.A. Holmberg, Y.S. Yan, Synthesis of template-free zeolite nanocrystals by using thermoreversible polymer hydrogels, Journal of the American Chemical Society 125 (2003) 9928–9929.
[23] D. Li, Y. Huang, K.R. Ratinac, S.P. Ringer, H. Wang, Zeolite crystallization in crosslinked chitosan hydrogels: crystal size control and chitosan removal, Microporous and Mesoporous Materials 116 (2008) 416–423.
[24] L. Li, P.M. Thangamathesvaran, C.Y. Yue, Gel network structure of methylcellulose in water, Langmuir 17 (26) (2001) 8062–8068.
[25] A. Charkhi, M. Kazemeini, S.J. Ahmadi, H. Kazemian, Fabrication of granulated NaY zeolite nanoparticles using a new method and study the adsorption properties, Powder Technology 231 (2012) 1–6.
[26] W.H. Flank, Properties of synthesized, ion-exchanged, and stabilized zeolite Rho, in: J.R. Katzer (Ed.), Molecular Sieves II—ACS Symposium Series, vol. 40, American Chemical Society, Washington, DC, 1977, pp. 43–52.